CrystEngComm

Two dimensional porous 3d–4f heterometallic coordination polymers constructed from pyridine-2,3-dicarboxylic acid

Journal:	*CrystEngComm*
Manuscript ID:	CE-ART-01-2015-000009.R3
Article Type:	Paper
Date Submitted by the Author:	16-Apr-2015
Complete List of Authors:	Yang, Ting-Hai; Jiangsu University of Technology, School of Chemistry & Environmental Engineering; University of Aveiro, Department of Chemistry Silva, Ana Rosa; University of Aveiro, Chemistry, CICECO; Unilever Discover Port Sunlight, Structured Materials Expertise Group SHI, Fa-Nian; University of Aveiro, Department of Chemistry, CICECO

CrystEngComm RSCPublishing

ARTICLE

Two dimensional porous 3*d*–4*f* heterometallic coordination polymers constructed from pyridine-2,3-dicarboxylic acid

Cite this: DOI: 10.1039/x0xx00000x

Received 00th January 2015,
Accepted 00th January 2015

DOI: 10.1039/x0xx00000x

www.rsc.org/

Ting-Hai Yang, *[a,c] Ana Rosa Silva [c] and Fa-Nian Shi*[b,c]

Reactions of pyridine-2,3-dicarboxylic acid ($pydcH_2$), cobalt acetate and lanthanide nitrate under hydrothermal conditions result in four new 3*d*-4*f* heterometallic coordination polymers, namely, $[LnCo(pydc)_3(H_2O)_3]\cdot 9H_2O$ {Ln = Dy (**1**), Ho (**2**), Er (**3**) and Tm (**4**)}. All compounds were characterized by elemental analysis, IR spectroscopy, SEM, EDS, thermal gravimetric analysis and X-ray diffraction. The compounds feature a two dimensional (2-D) layer structure with large apertures, in which each $pydc^{2-}$ ligand links two metal centers and each metal center was bonded to three $pydc^{2-}$ and vice versa. The adsorption and catalytic properties of compound **1** were investigated.

Introduction

The synthesis and characterization of transition metal-lanthanide (3*d*-4*f*) heterometallic coordination polymers (TMLnCPs) are one of the most attractive areas of material research.[1-4] The great interests in this area are driven by not only their fascinating architectures and topologies but also the potential applications in luminescence,[5-10] magnetism,[11-19] adsorption[20-23] and catalysis.[24-27] However, novel 3*d*-4*f* TMLnCPs are difficult to obtain, due to the reason that the competing reaction of transition metals (TM) and lanthanides (Ln) occurs to the same ligand. These complicated competing reactions very often lead to the generation of preferably homometallic complexes instead of heterometallic ones.

On the basis of the hard-and-soft-acid-base theory, it seems feasible to use N/O mixed ligands for synthesizing TMLnCPs. The *f*-block ions behave as hard acids and prefer O-donors to N-donors, while *d*-block metal ions have a strong tendency to coordinate to both N- and O-donors.[19] Pyridine-2,3-dicarboxylic acid ($pydcH_2$) is one of the excellent N/O mixed ligands for construction of TMLnCPs due to its coordination behaviours that serve as a bridge between Ln and TM ions. However, to the best of our knowledge, only a limited number of 3*d*-4*f* coordination polymers[22,28-33] based on pyridine-2,3-dicarboxylic acid have been reported.

On the other hand, porous coordination polymers have attracted much interest for their potential as adsorption materials and catalysts due to their high surface areas with well-defined pore properties, easily tunable and tailorable structures and chemical functionality, which facilitate diffusion and the interfacial contact between the active site and the reagents.[34-38] Recently, we have reported that a series of novel porous TMLnCPs based on 3,5-pyrazole dicarboxylic acid[25] were an active and recyclable heterogeneous catalysts in the cyclopropanation of styrene. Inspired by these results, we wondered whether it is possible to use other N/O mixed ligand to construct porous 3*d*-4*f* TMLnCPs with similar functions. As a result, we used a one-pot reaction to assemble four new 3*d*-4*f* TMLnCPs, $[LnCo(pydc)_3(H_2O)_3]\cdot 9H_2O$ {Ln = Dy (**1**), Ho (**2**), Er (**3**) and Tm (**4**)}, based on pyridine-2,3-dicarboxylic acid ligand, which exhibit a 2-D layer structure with large apertures. In addition, the stability, adsorption and catalytic properties were also investigated.

Experimental

Materials and methods

All the other starting materials were of reagent quality and were obtained from commercial sources without further purification. Elemental analyses for C, N and H were performed on a TruSpec 630-200-200 elemental analyser with a combustion furnace temperature of 1075 °C and an afterburner temperature of 850 °C. FT-IR spectra were collected from KBr pellets (Aldrich 99%+, FT-IR grade) on a Mattson 7000 FT-IR spectrometer in a range of 4000–400 cm^{-1} at the resolution of 2 cm^{-1}. Thermogravimetric analyses (TGA) were carried out using a Shimadzu TGA 50 under air, from room temperature to ca. 700 ºC, with a heating rate of 10 ºC/min. Powder X-ray diffraction (PXRD) patterns were recorded at ambient temperature using an Empyrean diffractometer with Cu-Kα radiation (λ = 1.54178 Å) in the 2θ range of 5 to 50° in reflection mode, which is equipped with a X'Celerator detector, a curved graphite-monochromated radiation and a flat-plate sample holder, in a Bragg-Brentano para-focusing optics configuration (45 kV, 40 mA). Scanning electron microscopy (SEM) and energy dispersive analysis of X-ray spectroscopy (EDS) were performed using a Hitachi S-4100 field emission gun tungsten filament instrument working at 25 kV. Samples were prepared by deposition on aluminium sample

holders with carbon coating. Nitrogen sorption experiments were carried out on a Micrometrics Gemini2380 volumetric gas sorption instrument. Prior to N_2 isotherm measurements at 77 K, the sample was outgassed under a high vacuum at 120 °C for 18 h and was weighed before and after the degassing procedure to confirm the evacuation of the solvents.

In the catalytic experiments, the synthesis of cyanohydrins was performed using 1.64 mmol of benzaldehyde, 0.99 mmol of chlorobenzene (internal standard), 1.80 mmol of trimethylsilane cyanide (TMSCN), 0.0527 g of **1**, previously dried at 120°C under vacuum, in 5.00 mL of dichloromethane, under inert atmosphere at room temperature. The reaction was followed by GC using a Bruker 450 GC gas chromatograph equipped with a fused silica Varian Chrompack capillary column VF-1 ms (15 m x 0.25 mm id; 0.25 µm film thickness) and a fused silica Varian Chrompack capillary column CP Chirasil-DEX (25 m x 0.25 mm id; 0.25 µm film thickness), using helium as carrier gas. Conditions used: 100°C (30 min); injector temperature, 200°C; detector temperature, 230°C. The obtained products were confirmed using a Finnigan Trace GC-MS.

Synthesis of compounds $[LnCo(pydc)_3(H_2O)_3]\cdot 9H_2O$ {Ln = Dy (1), Ho (2), Er (3) and Tm (4) }

Compounds **1-4** were obtained under the same experimental conditions. In a general synthesis, a mixture containing $pydcH_2$ (0.60 mmol, 0.1002 g), $Co(OAc)_2\cdot 4H_2O$ (0.20 mmol, 0.4981 g) and $Dy(NO_3)_3\cdot 6H_2O$ (0.20 mmol, 0.0912 g) [or $Ho(NO_3)_3\cdot 6H_2O$ (0.0916 g) or $Er(NO_3)_3\cdot 6H_2O$ (0.0920 g) or $Tm(NO_3)_3\cdot 6H_2O$ (0.0924 g)] in 8 mL H_2O was kept in a Teflon-lined autoclave and placed inside a preheated oven at 120 °C for 72 h. After the autoclave was cooled to room temperature, purple-red needle-like crystals of compound **1** suitable for single-crystal X-ray diffraction analyses were isolated from final reaction products by filtration after washing several times with distilled water, and dried in air at ambient temperature. The purities of the samples were confirmed by powder X-ray diffraction studies and elemental analyses.

For **1**, Yield: 59 mg, 32%. Anal. calcd for $C_{21}H_{33}O_{24}N_3CoDy$: C, 27.03; H,3.57; N, 4.50%. Found: C, 26.92; H, 3.65; N, 4.31%. IR (KBr, cm^{-1}): 3410(br), 1671(s), 1604(s), 1566(s), 1478(w), 1422(s), 1348(s), 1278(m), 1238(w), 1178(w), 1159(w), 1122(m), 1075(w), 890(m), 865(w), 830(w), 745(m), 697(m), 564(w), 501(m), 371(w), 314(m).

For **2**, Yield: 56 mg, 30%. Anal. Found (calcd) for $C_{21}H_{33}O_{24}N_3CoHo$: C, 26.97; H, 3.56; N, 4.49%. Found: C, 26.86; H, 3.66; N, 4.36%. IR (KBr, cm^{-1}): 3422(br), 1669(s), 1600(s), 1568(s), 1479(w), 1421(s), 1349(s), 1276(m), 1238(w), 1178(w), 1158(w), 1121(m), 1074(w), 891(m), 864(w), 832(w), 743(m), 695(m), 566(w), 504(m), 377(w), 317(m).

For **3**, Yield: 54 mg, 29%. Anal. Found (calcd) for $C_{21}H_{33}O_{24}N_3CoEr$: C, 26.90; H, 3.55; N, 4.48%. Found: C, 26.76; H, 3.66; N, 4.39%. IR (KBr, cm^{-1}): 3413(br), 1669(s), 1600(s), 1568(s), 1481(w), 1420(s), 1348(s), 1278(m), 1236(w), 1179(w), 1158(w), 1122(m), 1077(w), 891(m), 863(w), 834(w), 743(m), 695(m), 565(w), 504(m), 377(w), 316(m).

For **4**, Yield: 29 mg, 16%. Anal. Found (calcd) for $C_{21}H_{33}O_{24}N_3CoTm$: C, 26.85; H, 3.54; N, 4.47%. Found: C, 26.78; H, 3.65; N, 4.39 %. IR (KBr, cm^{-1}): 3422(br), 1670(s), 1602(s), 1569(s), 1480(w), 1421(s), 1345(s), 1275(m), 1236(w), 1178(w), 1158(w), 1120(m), 1073(w), 889(m), 863(w), 831(w), 745(m), 696(m), 564(w), 503(m), 373(w), 317(m).

X-ray crystallographic analysis

Single crystals with dimensions 0.16×0.10×0.08 mm for **1**, 0.52×0.16×0.12 mm for **2**, 0.46×0.14×0.12 mm for **3** and 0.42×0.10×0.08 mm for **4** were selected for indexing and intensity date collection at 150 K on a Bruker SMART APEX-II CCD diffractometer equipped with graphite-monochromatized Mo Kα (λ = 0.71073Å) radiation. The low temperature was served by an Oxford Cryostems Series 700 cryostream monitored remotely by using the software interface Cryopad. A hemisphere of data was collected in the θ range 1.79-25.99° for **1**, 1.80-20.52° for **2**, 3.12-30.50° for **3** and 3.13-30.54° for **4** using a narrow-frame method with scan widths of 0.30° in ω and an exposure time of 10s per frame. Numbers of measured and observed reflections [$I > 2\sigma(I)$] are 6913 and 2099 (R_{int} = 0.0345) for **1**, 6602, 3194 (R_{int} = 0.0370) for **2**, and 6528 and 3003 (R_{int} = 0.0341) for **3** and 6498 and 3146 (R_{int} = 0.0375) for **4** respectively. The data were integrated using the Siemens SAINT program,[39] with the intensities corrected for Lorentz factor, polarization, air absorption, and absorption due to variation in the path length through the detector faceplate.

Table 1 Crystallographic data for compounds **1- 4**

Compound	**Dy**	**Ho**	**Er**	**Tm**
Empirical formula	$C_{21}H_{33}O_{24}N_3CoDy$	$C_{21}H_{33}O_{24}N_3CoHo$	$C_{21}H_{33}O_{24}N_3CoEr$	$C_{21}H_{33}O_{24}N_3CoTm$
F. w.	932.85	935.35	937.68	939.35
Crystal system	Trigonal	Trigonal	Trigonal	Trigonal
Space group	P3	P3	P3	P3
$a = b$ (Å)	13.1350(10)	13.0601(3)	13.0479(3)	13.0373(3)
c (Å)	5.8794(12)	5.8637(3)	5.8596(2)	5.8491(3)
$\alpha = \beta$ (°)	90	90	90	90
γ (°)	120	120	120	120
V(Å^3)	878.5(2)	866.15(5)	863.93(4)	860.98(5)
Z	1	1	1	1
D_c (g/cm^3)	1.440	1.482	1.491	1.499
μ (mm^{-1})	2.641	2.806	2.952	3.102
F(000)	366	376	377	378
GOF on F^2	1.003	1.000	1.001	1.002
R_1, wR_2 [a]	0.0222,	0.0291,	0.0299,	0.0329,
[$I > 2\sigma(I)$]	0.0566	0.0581	0.0606	0.0666
R_1, wR_2 [a]	0.0223,	0.0297,	0.0304,	0.0336,
(All date)	0.0566	0.0583	0.0609	0.0669
(Δρ)max,	0.242,	0.750,	1.060,	1.035,
(Δρ)min (eÅ^{-3})	-0.370	-0.704	-0.479	-0.505

[a] $R_1 = \Sigma||F_o| - |F_c||/\Sigma|F_o|$, $wR_2 = [\Sigma w(F_o^2 - F_c^2)^2/\Sigma w(F_o^2)^2]^{1/2}$

The structures were solved by direct method using SHELXS-97[40] and refined on F^2 by full matrix least-squares using SHELXL-97.[41] All the non-hydrogen atoms were refined anisotropically. All H atoms were refined isotropically. Identification of solvent entities was impossible for **1**−**4** complexes because of disorder contents of the large pores, so squeeze refinements have been performed using PLATON.[42] Crystallographic and refinement details are listed in Table 1. Selected bond lengths are given in Tables 2. CCDC reference numbers: 1040740-1040743 correspond to compounds **1**, **2**, **3** and **4**, respectively.

Table 2 Selected bond lengths (Å) for **1-4**.

	1(Dy)	2(Ho)	3(Er)	4(Tm)
Co(1)-O(1)	1.888(3)	1.876(3)	1.893(3)	1.889(3)
Co(1)-N(1)	1.925(4)	1.916(3)	1.923(3)	1.921(3)
Ln(1)-O(3)	2.402(3)	2.416(3)	2.403(3)	2.395(3)
Ln(1)-O(4)	2.472(3)	2.486(3)	2.451(3)	2.457(3)
Ln(1)-O(5)	2.334(3)	2.356(3)	2.327(3)	2.311(3)
C(6)-O(1)	1.296(5)	1.273 (4)	1.288(5)	1.279(5)
C(6)-O(2)	1.200(6)	1.222(5)	1.221(5)	1.233(5)
C(7)-O(3)	1.271(6)	1.279(5)	1.276(5)	1.273(5)
C(7)-O(4)	1.276(6)	1.262(5)	1.258(5)	1.257(5)

Sysmmerty codes: A: -x+y+1,-x+1,z, -z+5/3; B: -y+1,x-y,z; C: -y+2,x-y+1,z; D: -x+y+1,-x+2,z.

Results and discussion

Description of Structures

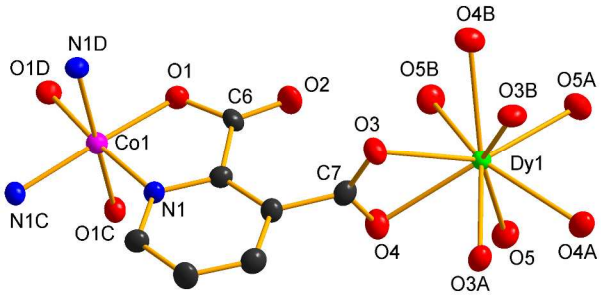

Fig. 1 Building unit of **1** with the atomic labelling scheme (30% probability). All H atoms were omitted for clarity. Symmetry codes are the same as those given in Table 2.

Compounds **1**-**4** are isostructural, crystallized in trigonal lattice with *P3* space group. Hence only the structure of **1** will be discussed in detail as representative. The asymmetric unit of **1** consists of one-third Co^{3+} ion, one-third Dy^{3+} ion, one $pydc^{2-}$ ligand, one coordinated water and three disorder lattice water molecules that were identified by thermal gravimetric analyses. As shown in Fig. 1, the Co^{3+} ion has a distorted octahedral environment, surrounded by three carboxylate oxygen atoms[O(1), O(1C), O(1D)] and three pyridyl nitrogen atoms[N(1), N(1C), N(1D)] from three equivalent $pydc^{2-}$ ligand. The Co–O and Co–N bond lengths are 1.888(3) Å and 1.925(4) Å, respectively (Table 2). The Dy^{3+} ion is nine-coordinated and has distorted tricapped trigonal prismatic coordination environment with Dy(1) being bonded by three water molecules [O(5), O(5A), O(5B)] and six carboxylate oxygen atoms [O(3), O(4), O(3A), O(4A), O(3B), O(4B)] from three equivalent $pydc^{2-}$ ligand. The Dy–O bond lengths fall in the range 2.334(3) and 2.472(3) Å, which are comparable to the reported compounds, $[CuDy_2(pdc)_2(Hpdc)(H_2O)_4]\cdot 2H_2O$[25], {[DyZn(pydc)2(L)$(H_2O)_8$] $7H_2O$}[25, 30].

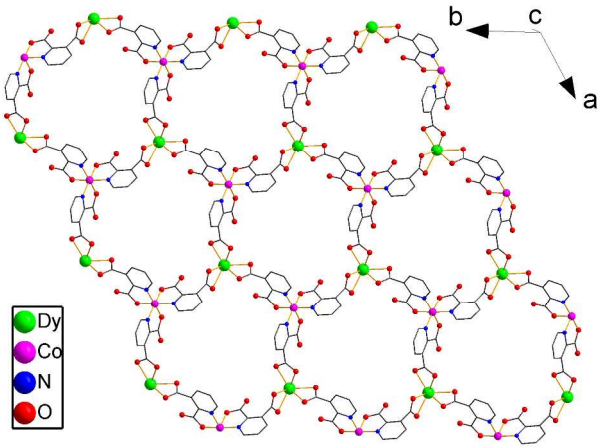

Fig.2 Layer porous structure of **1**. All water molecules and H atom are omitted for clarity.

The $pydc^{2-}$ ligand chelates the Co^{3+} and Dy^{3+} ions in μ_4-η^2N, O, η^2O', O'' fashion through O1, N1 and O3, O4 atoms (Fig. 1), respectively, bridging the Co^{3+} and Dy^{3+} ions via pyridyl group. As a result, each $pydc^{2-}$ ligand links two metal centers and each metal center is bonded via three $pydc^{2-}$ and vice versa, thus forming a two-dimensional layered structure in the *ab* plane with large apertures bound by six metal ions and six $pydc^{2-}$ ligands of $[Co_3Dy_3(pydc^{2-})_6]$(Fig. 2).

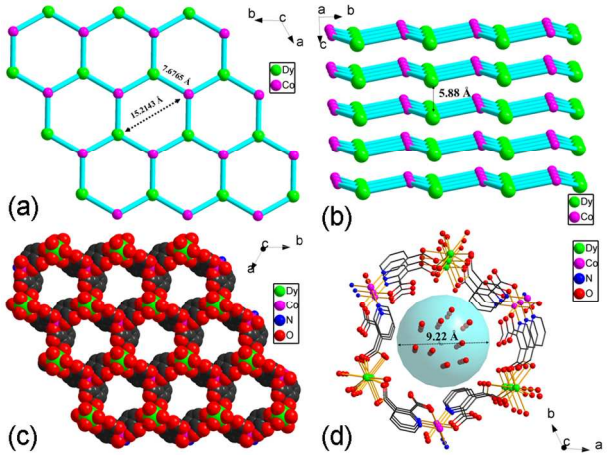

Fig. 3 (a) The layer topology structure of **1**; (b) The packing topology of **1**; (c) 3D pore space-fill structure of **1**; (d) The packing structure of **1**, the red dots are guest water molecules.

If each metal center is taken as a node, each Co atom is surrounded by three Dy atoms and vice versa, resulting in a 3-connected uninodal honeycomb (*hcb*) topology layer, with the point

symbol of $\{6^3\}$ on the basis of the TOPOS 4.0 program.[43] The Co···Dy distances across one and three $pydc^{2-}$ bridges are 7.6765 and 15.2143 Å respectively (Fig.3(a)). The interlayer distance is 5.81 Å.

The 2D layers are further linked together in the type of *AAA*… fashion along *c* axis (Fig.3(b)), give rise to a 3-D porous structure (Fig.3(c)) through interlayer hydrogen bonds (Fig. S1) with the O5···O3 hydrogen bonding distances of 2.71 Å (Table S1). The distance between two neighbour layers is 5.88 Å (Fig. 3b). The pores, with the size of about 9.22 Å free diameter, are filled with disordered lattice H_2O molecules (Fig.3(d)).

The structures of compounds **2**-**4** are analogous to **1** except that the Dy^{3+} ion in **1** is replaced by Ho^{3+} in **2**, Er^{3+} in **3** and Tm^{3+} in **4**. The cell volumes decrease in turn from **1** to **4**, in accordance with the decreasing sequence of the ionic radii of the corresponding metal ions due to the lanthanide contraction.

Synthesis and IR Spectra

The IR spectra for compounds **1**−**4** were recorded in the region from 4000−400 cm^{-1}. The presence of lattice and coordination water molecules is manifested by a broad IR band of medium intensity in the range of about 3500 cm^{-1}, assigned to ν(OH). No strong absorption peaks ranging from 1690 to 1730 cm^{-1} for –COOH are observed in compounds **1**–**4**, confirming that all carboxyl groups of H_2pydc ligand are deprotonated, which agrees with the single X-ray crystal structure analyses. The strong peaks at 1670–1270 cm^{-1} are assigned to the asymmetric and symmetric vibrations of the coordinated carboxylate groups (Fig. S2−S5).

SEM, EDS and PXRD

Scanning electron microscopy (SEM, Fig.4) shows particles with an almost similar crystal habits with the shape of long prism for all compounds. EDS analysis (Fig.S6-S9) gave the molar ratios Co: Dy = 1 : 1 for (**1**), Co : Ho= 1 : 1 for (**2**), Co : Er = 1 : 1 for (**3**) and Co : Tm = 1 : 1 for (**4**), in good agreement with the molecular formulae derived from the single crystal structures.

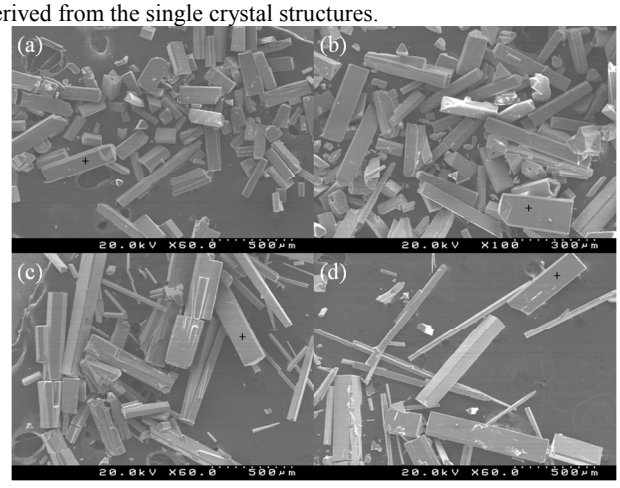

Fig. 4 SEM images of (a) **1**, (b) **2**, (c) **3** and (d) **4**

The experimental and simulated powder X-ray diffraction (PXRD) patterns of complexes **1**–**4** are shown in Fig. 5. The experimental PXRD patterns at room temperature are in good agreement with the simulated ones based on the single crystal X-ray solution. Furthmore, the diffraction peaks of compounds **1**−**4** can be refined by using TOPAS program,[44] resulting in a similar cell parameters to single crystal analysis (Fig. S10-S13 and Table S2).

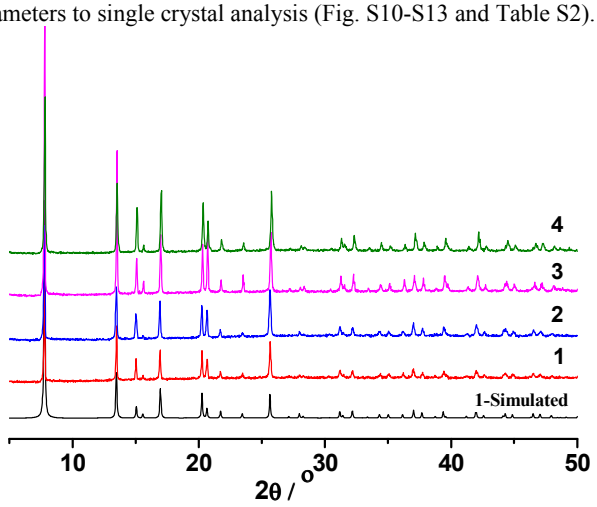

Fig. 5. Experimental and simulated PXRD patterns of **1**-**4**.

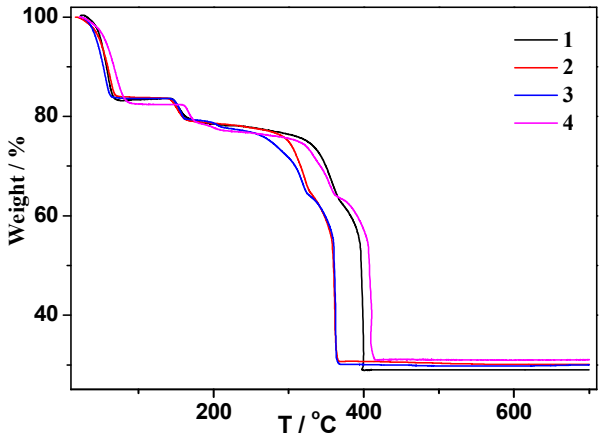

Fig. 6 TG curves of complexes **1**–**4**.

Thermal stability

Thermal gravimetric analyses (TG) were carried out for **1**–**4** to examine the thermal stabilities of these complexes in air (Fig. 6). The TG curves of **1**–**4** display similar four stage weight loss process from 20 to 700 °C which indicates that **1**–**4** have analogical thermal stability due to their isomorphic structures. The first weight loss is accompanied by the loss of all lattice water molecules in the temperature range of 25–120 °C (calcd, found: 17.4, 16.5% for **1**, 17.3, 16.3% for **2**, 17.3, 16.4% for **3** and 17.3, 17.5% for **4**). Further weight loss between 120 and 240 °C correspond to the release of the coordinated water molecules (calcd, found: 5.8, 6.0% for **1**, 5.8, 6.1% for **2**, 5.8, 6.4% for **3** and 5.8, 5.7% for **4**). The other two steps of weight losses above 240 °C are due to the decomposition of

pydc^{2-} fragments and the collapse of the lattice structure. The final residues were not further characterized. Indeed, in situ variable-temperature powder X-ray diffraction studies of **1** (Fig. 7) reveal that the structure starts to change between 125–150 °C. The weight losses observed up to ca. 125 °C are attributed to the gradual release of the disorder lattice water molecules from the structure pores

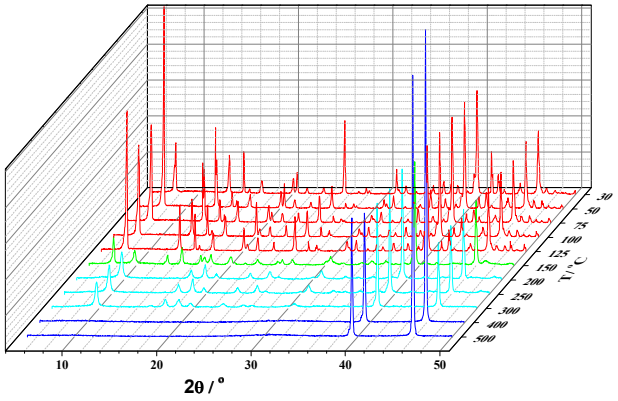

Fig. 7 In situ variable-temperature powder X-ray diffraction patterns of **1** between 30 and 500 °C.

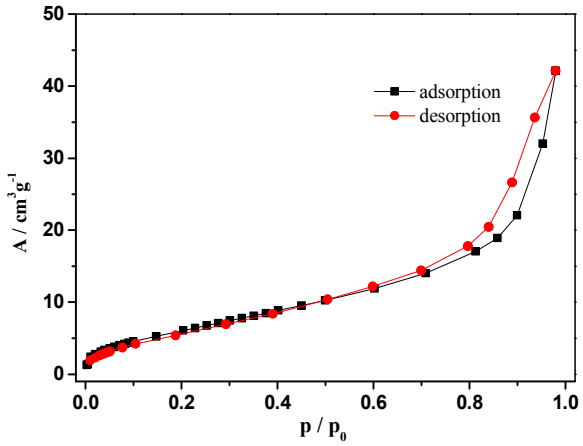

Fig. 8 Adsorption/desorption isotherm of N_2 gas (77 K) for **1**.

Gas Sorption property

As discussed above, 1-D channels with the size of about 9.22 Å free diameter were observed along *c* axis [Fig 3(c)] in compound **1**. Furthermore, compound **1** has a total potential solvent accessible void of 344.8 Å^3 calculated by PLATON analysis,[42] which approximately corresponds to 39.3% of the crystal volume (878.5 Å^3) after removing the lattice water molecules. The compound **1** can keep its crystalline nature even under the condition of more than 125 °C based on the in situ variable-temperature PXRD (Fig. 7). Before gas adsorption tests, the activation for removing the guest molecules from the pores by heating the sample under vacuum is required and the as-synthesized sample was heated at an optimized temperature of 120 °C for 18 h. The N_2 adsorption isotherms for **1** at 77 K are shown in Fig. 8. The permanent porosity of **1** was confirmed by its N_2 adsorption/desorption isotherm, which displayed typical Type-III gas sorption behavior[45] and a nitrogen gas uptake of approximately 42 cm^3(STP)/g at p/p_0= 0.95 and a BET surface area of 22 m^{2}g^{-1}. Therefore, these TMLnCPs may be suitable candidates for porous materials.

Catalytic property

One of the most common applications of MOFs is as heterogeneous catalysts of organic reactions. We have been studying the catalytic activity of novel MOF and coordination polymer structures in several organic transformations.[25-27] The Co(II) centers of compound **1** are fully coordinated with non labile ligands and should not be catalytic active. On the other hand, the coordination number of the Dy(III) centers is 9, but possess water labile ligands. A reaction that has been described to be catalyzed by MOFs with lanthanides as active centers was thus chosen.[46,47] The catalytic activity of compound **1** was tested in the synthesis of cyanohydrins at room temperature (Fig. 9). The MOF showed catalytic activity in the conversion of benzaldehyde (29±6%) with TMSCN into the corresponding cyanohydrin with high selectivity (96%) in just 3.4% mol. Trimethylsilyl benzoate was obtained as by-product. 2-methoxybenzaldehyde could also be converted into the corresponding cyanohydrin by compound **1** and TMSCN with high selectivity (almost 100%), but lower conversion (10%), in 3.3% mol and the same amount of time. This may be due to both electronic and steric effects of the methoxy group.[46] *o*-tolualdehyde cyanohydrin could also be synthesized using TMSCN (29%) and compound **1** with high selectivity (98%). It is noteworthy that no significant aldehyde conversion could be observed without the addition of compound **1**. As reported earlier for MOFs containing lanthanides,[46,47] the Dy(III) should be the catalytic active site, probably via displacement of the labile water molecules by aldehyde before its activation and reaction. No enantiomeric induction was observed in both cyanohydrins, despite of the MOF structure belonging to a chiral space group. The MOF **1** was filtered from the reaction media and after convenient washing and drying, it was reused in another catalytic cycle. It showed again catalytic activity in the synthesis of benzaldehyde cycanohydrin with high selectivity (93%), but with lower conversion for the same reaction time (9%).

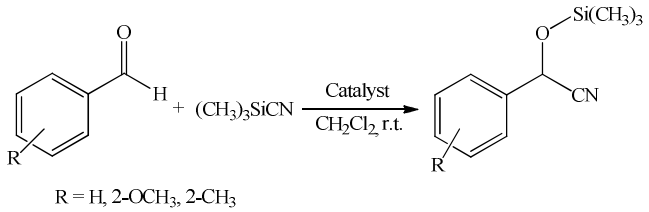

Fig. 9 Synthesis of cyanohydrins at room temperature.

Conclusions

In summary, four new 3*d*–4*f* heterometallic TMLnCPs with the molecular formula $[LnCo(pydc)_3(H_2O)_3]\cdot 9H_2O$ {Ln = Dy (**1**), Ho (**2**), Er (**3**) and Tm (**4**)} were synthesized hydrothermally. These compounds exhibit a 2-D layer structure with large apertures, in which each $pydc^{2-}$ ligand links two metal centers and each metal centers are bonded by three $pydc^{2-}$ and vice versa. The N_2 gas adsorption property of compound **1** shows that the TMLnCPs may be suitable as candidates for porous materials. The catalytic properties of **1** show that it is active in the synthesis of benzaldehyde cyanohydrin , and other aldehydes, with high selectivity.

Acknowledgements

We thank Fundação para a Ciência e a Tecnologia (FCT), FEDER, QREN, COMPETE (PEst-C/CTM/LA0011/2013) and (FCT: SFRH/BPD/ 74582/2010) for financial support. F.-N. SHI acknowledges FCT for the project of PTDC/CTM-NAN/119994/2010. T.-H. Yang acknowledges the NSF of Jiangsu Province (BK20140244), The Project Sponsored by the Scientific Research Foundation for Returned Overseas Chinese Scholars of State Education Ministry, the NSF for Universities in Jiangsu Province (13KJB150013), the Science and Technology Bureau of Changzhou City (No. CJ20140031) and Jiangsu University of Technology(KYY13035). We also thank Dr. Song-Song Bao (College of Chemistry and Chemical Engineering at Nanjing University of China) for his help in refining PXRD data.

Notes and references

[a] School of Chemistry & Environmental Engineering, Jiangsu University of Technology, Changzhou 23001, P R China. Fax: +86-519-86953269; Tel: +86-519-86953269; E-mail: tinghai_yang@hotmail.com, fshi@ua.pt.
[b] School of Science, Shenyang University of Technology, 110870, Shenyang, P R China.
[c] Department of Chemistry, CICECO, University of Aveiro, 3810-193 Aveiro, Portugal.

† Electronic Supplementary Information (ESI) available: IR data, EDS, P-XRD and table of hydrogen bonding interaction data of **1**. CCDC 1040740-1040743. For ESI and crystallographic data in CIF or other format see DOI: 10.1039/b000000x/

1 C. Benelli and D. Gatteschi, *Chem. Rev.*, 2002, **102**, 2369-2387.
2 M. Sakamoto, K. Manseki and H. Okawa, *Coord. Chem. Rev.*, 2001, **219**, 379-414.
3 C. E. Plecnik, S. M. Liu and S. G. Shore, *Accounts Chem Res*, 2003, **36**, 499-508.
4 J.-L. Liu, Y.-C. Chen, F.-S. Guo and M.-L. Tong, *Coord. Chem. Rev.*, 2014, **281**, 26-49.
5 R. Feng, L. Chen, Q.-H. Chen, X.-C. Shan, Y.-L. Gai, F.-L. Jiang and M.-C. Hong, *Cryst. Growth Des.*, 2011, **11**, 1705-1712.
6 X. D. Zhu, Z. J. Lin, T. F. Liu, B. Xu and R. Cao, *Cryst. Growth Des.*, 2012, **12**, 4708-4711.
7 L. Liang, G. Peng, L. Ma, L. Sun, H. Deng, H. Li and W. S. Li, *Cryst. Growth Des.*, 2012, **12**, 1151-1158.
8 G. Peng, L. Ma, L. Liang, Y. Z. Ma, C. F. Yang and H. Deng, *CrystEngComm*, 2013, **15**, 922-930.
9 Q. B. Bo, H. Y. Wang, D. Q. Wang, Z. W. Zhang, J. L. Miao and G. X. Sun, *Inorg. Chem.*, 2011, **50**, 10163-10177.
10 X. P. Yang, C. Chan, D. Lam, D. Schipper, J. M. Stanley, X. Y. Chen, R. A. Jones, B. J. Holliday, W. K. Wong, S. C. Chen and Q. Chen, *Dalton Trans.*, 2012, **41**, 11449-11453.
11 J. S. Shim and J. O. Liu, *Int. J. Biol. Sci.*, 2014, **10**, 654-663.
12 J.-B. Peng, Q.-C. Zhang, X.-J. Kong, Y.-P. Ren, L.-S. Long, R.-B. Huang, L.-S. Zheng and Z. Zheng, *Angew. Chem., Int. Ed.*, 2011, **50**, 10649-10652.
13 J. Rinck, G. Novitchi, W. Van den Heuvel, L. Ungur, Y. Lan, W. Wernsdorfer, C. E. Anson, L. F. Chibotaru and A. K. Powell, *Angew. Chem., Int. Ed.*, 2010, **49**, 7583-7587.
14 P. F. Shi, G. Xiong, B. Zhao, Z. Y. Zhang and P. Cheng, *Chem. Commun.*, 2013, **49**, 2338-2340.
15 J. B. Peng, Q. C. Zhang, X. J. Kong, Y. Z. Zheng, Y. P. Ren, L. S. Long, R. B. Huang, L. S. Zheng and Z. P. Zheng, *J. Am. Chem. Soc.*, 2012, 134, 3314-3317.
16 Y. H. Su, S. S. Bao and L. M. Zheng, *Inorg. Chem.*, 2014, 53, 6042-6047.
17 S. M. T. Abtab, M. Maity, K. Bhattacharya, E. C. Sanudo and M. Chaudhury, *Inorg. Chem.*, 2012, 51, 10211-10221.
18 H. Xiang, W. G. Lu, W. X. Zhang and L. Jiang, *Dalton Trans.*, 2013, **42**, 867-870.
19 Q. Yue, J. Yang, G. H. Li, G. D. Li, W. Xu, J. S. Chen and S. N. Wang, *Inorg. Chem.*, 2005, **44**, 5241-5246.
20 Y. Wang, P. Cheng, J. Chen, D.-Z. Liao and S.-P. Yan, *Inorg. Chem.*, 2007, **46**, 4530-4534.
21 C. J. Li, Z. J. Lin, M. X. Peng, J. D. Leng, M. M. Yang and M. L. Tong, *Chem. Commun.*, 2008, 6348-6350.
22 H.-M. Peng, H.-G. Jin, Z.-G. Gu, X.-J. Hong, M.-F. Wang, H.-Y. Jia, S.-H. Xu and Y.-P. Cai, *Eur. J. Inorg. Chem.*, 2012, 5562-5570.
23 M. Fang, B. Zhao, Y. Zuo, J. Chen, W. Shi, J. Liang and P. Cheng, *Dalton Trans*, 2009, 7765-7770.
24 O. V. Amirkhanov, O. V. Moroz, K. O. Znovjyak, T. Y. Sliva, L. V. Penkova, T. Yushchenko, L. Szyrwiel, I. S. Konovalova, V. V. Dyakonenko, O. V. Shishkin and V. M. Amirkhanov, *Eur. J. Inorg. Chem.*, 2014, 3720-3730.
25 T.-H. Yang, A. R. Silva and F.-N. Shi, *Dalton Trans.*, 2013, **42**, 13997-14005.
26 F. N. Shi, A. R. Silva, T. H. Yang and J. Rocha, *CrystEngComm*, 2013, **15**, 3776-3779.
27 F.-N. Shi, A. R. Silva and L. Bian, *J Solid State Chem*, 2015, 225, 45-52.
28 P. Mahata, G. Sankar, G. Madras and S. Natarajan, *Chem. Commun.*, 2005, 5787-5789.
29 M. Li, J. F. Xiang, L. J. Yuan, S. M. Wu, S. P. Chen and J. T. Sun, *Cryst. Growth Des.*, 2006, **6**, 2036-2040.
30 S. J. Liu, J. M. Jia, Y. Cui, S. D. Han and Z. Chang, *J Solid State Chem*, 2014, **212**, 58-63.
31 L. Du, R. B. Fang and Q. H. Zhao, *Chinese J Chem*, 2008, 26, 957-961.
32 N. Wang, S. T. Yue, H. Y. Wu, Z. Y. Li, X. X. Li and Y. L. Liu, *Inorg. Chim. Acta*, 2010, **363**, 1008-1012.
33 S. J. Liu, W. C. Song, L. Xue, S. D. Han, Y. F. Zeng, L. F. Wang and X. H. Bu, *Sci. China Chem.*, 2012, 55, 1064-1072.

34 J. R. Li, J. Sculley and H. C. Zhou, *Chem. Rev.*, 2012, **112**, 869-932.
35 H. H. Wu, Q. H. Gong, D. H. Olson and J. Li, *Chem. Rev.*, 2012, **112**, 836-868.
36 L. E. Kreno, K. Leong, O. K. Farha, M. Allendorf, R. P. Van Duyne and J. T. Hupp, *Chem. Rev.*, 2012, **112**, 1105-1125.
37 J. R. Li, R. J. Kuppler and H. C. Zhou, *Chem. Soc. Rev.*, 2009, **38**, 1477-1504.
38 J. Lee, O. K. Farha, J. Roberts, K. A. Scheidt, S. T. Nguyen and J. T. Hupp, *Chem. Soc. Rev.*, 2009, **38**, 1450-1459.
39 *SAINT+, Data Integration Engine, v. 7.23a*, Bruker AXS, Madison, Wisconsin, 1997-2005.
40 G. M. Sheldrick, *SHELXS-97, Program for Crystal Structure Solution*, University of Göttingen, Germany, 1997.
41 G. M. Sheldrick, *SHELXL-97, Program for Crystal Structure Refinement*, University of Göttingen, Germany, 1997.
42 A. L. Spek, *PLATON,A Multipurpose Crystallographic Tool*, Utrecht University Utrecht, 2007.
43 V. A. Blatov and A. P. Shevchenko, *TOPOS–Version Professional beta evaluation*, Samara State University, Samara, Russia, 2006.
44 *TOPAS*, *Version 4.2*, Bruker AXS GmbH, Karlsruhe, Germany, 2009.
45 S. Kitagawa, R. Kitaura and S. Noro, *Angew. Chem., Int. Ed.*, 2004, **43**, 2334-2375.
46 Y. Zhu, Y. Wang, P. Liu, C. Xia, Y. Wu, X. Lu, J. Xie, *Dalton Trans.*, 2015, **44**, 1955–1961.
47 R. F. D Vries, V. A. de la Peña-O'Shea, N. Snejko, M. Iglesias, E. Gutiérrez-Puebla, M. Ángeles Monge, *Cryst. Growth Des.* 2012, **12**, 5535−5545.

Two dimensional porous 3*d*–4*f* heterometallic coordination polymers constructed from pyridine-2,3-dicarboxylic acid

Ting-Hai Yang,*[a,c] Ana Rosa Silva[c] and Fa-Nian Shi*[b,c]

[a] School of Chemistry & Environmental Engineering, Jiangsu University of Technology, Changzhou 23001, P R China. Fax: +86-519-86953269; Tel: +86-519-86953269; E-mail: tinghai_yang@hotmail.com, fshi@ua.pt.

[b] School of Science, Shenyang University of Technology, 110870, Shenyang, P R China.

[c] Department of Chemistry, CICECO, University of Aveiro, 3810-193 Aveiro, Portugal.

Synopsis

Four $Co^{III}Ln^{III}$ porous 3*d*–4*f* heterometallic coordination polymers with the $pydcH_2$ ligand were hydrothermally synthesized and characterized. The adsorption and catalytic properties of compound $Co^{III}Dy^{III}$ were investigated